

## A 36 W CW AlGaN/GaN-Power HEMT Using Surface-Charge-Controlled Structure

T.Kikkawa<sup>1</sup>, M.Nagahara<sup>2</sup>, T.Kimura<sup>1</sup>, S.Yokokawa<sup>2</sup>, S.Kato<sup>2</sup>, M.Yokoyama<sup>2</sup>, Y.Tateno<sup>2</sup>,

K.Horino<sup>2</sup>, K.Domen<sup>2</sup>, Y.Yamaguchi<sup>2</sup>, N.Hara<sup>1</sup>, and K.Joshin<sup>1</sup>

<sup>1</sup>Fujitsu Laboratories Ltd., 10-1 Morinosato-Wakamiya, Atsugi, Kanagawa, 243-0197, Japan

<sup>2</sup>Fujitsu Quantum Devices, 1000 Kamisukiawara, Nakakoma-Gun, Yamanashi, 409-3883, Japan

**Abstract** — We describe high power 36 W CW operation at 30 V using AlGaN/GaN HEMTs on SiC. Surface-charge-controlled structure, consisting of n-type doped thin GaN cap layer on AlGaN/GaN HEMT structure, is used to obtain high gate-drain breakdown voltage and to reduce current collapse. By optimizing threshold voltage of this structure, we obtained a maximum drain current of 1A/mm and a gate-drain breakdown voltage over 200 V. A 24-mm-wide-gate chip showed output power of 45.6 dBm (36 W) at 2.2 GHz with a liner gain of 9.7 dB.

### I. INTRODUCTION

AlGaN/GaN-based HEMTs are promising for microwave power applications, including L-band wireless base stations. There are many reports related to high output power density using a narrow gate device [1]. Pulsed measurements also exhibit high output power by suppressing heat generation [2]. Although continuous wave (CW) operation is required for high power application, a few papers reported total CW power over

30W using a wide gate chip [3]. This was because thermal problem occurred especially when a sapphire substrate was used. To solve a heat-sinking problem, a flip-chip or a SiC substrate has been considered. In this paper, we investigated GaN-HEMTs on SiC substrates and introduced the surface-charge-controlled structure [4], demonstrating a 36 W CW total output power.

To obtain higher RF-power and power added efficiency, we have to suppress frequency dependent characteristics, such as large transconductance ( $gm$ ) dispersion, gate-lag and current collapse [5-7]. We controlled the polarization-induced surface charge by n-type doping in a thin GaN cap on AlGaN and stabilized n-GaN-surface between electrodes using strongly stressed SiN [4]. This structure exhibited high off-state and on-state breakdown voltages of 200 V and 70 V with a maximum drain current of 1 A/mm. Recently, AlGaN-thickness effect began to be discussed [8]. In this paper, we studied the effect of threshold voltage ( $V_{th}$ ) on drain current,  $BV_{gd}$  and current collapse to obtain high output power with high

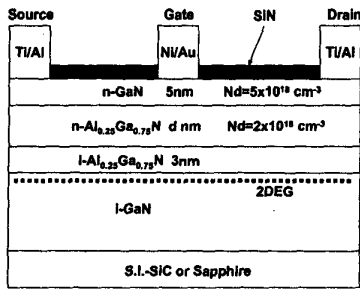


Fig.1. Schematic drawing of investigated surface-charge-controlled n-GaN-cap structures. Thin n-type GaN cap layer was grown on AlGaN/GaN conventional structure. Al mole fraction is 20-25%. SiN passivation was formed on GaN cap layer between electrodes. N-AlGaN thickness was varied to control  $V_{th}$ .

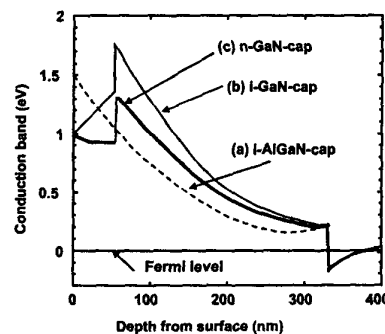


Fig. 2. Simulated band structure of (a) conventional AlGaN cap structure, (b) un-doped GaN cap structure and (c) novel surface-charge-controlled structure with thin n-GaN cap layer. N-GaN layer is 5 nm thick.



efficiency using surface-charge-controlled structure.

## II. EXPERIMENTAL

Figure 1 shows the device structures investigated (using in-house MOVPE grown Ga-face material on SiC substrates). N-AlGaN thickness was varied to change  $V_{th}$ . Mesa etching is used for isolation. Source/drain and gate electrodes were Ti/Al and Ni/Au. A stepper is used for gate lithography. Typical gate length is 0.9  $\mu\text{m}$ . A strongly stressed SiN was deposited on the n-GaN cap layer using plasma CVD after forming a gate electrode. Then, an air-bridged HEMT chip is fabricated. Gate width ( $W_g$ ) was varied from 40  $\mu\text{m}$  to 24 mm. After air-bridge fabrication, a 24-mm- $W_g$  chip was wire-bonded into a package with capacitors to obtain good impedance match.

## II. RESULTS AND DISCUSSION

### A. Surface-Charge-Controlled Structure on Sapphire

Figure 2 shows typical band diagram of the surface-charge-controlled structure (the n-GaN cap layer on  $\text{Al}_{0.20}\text{Ga}_{0.80}\text{N}/\text{GaN}$  HEMTs) compared with conventional structures. The surface-charge-controlled structure screens the polarization charges at GaN/AlGaN interface by 25% as shown in Fig.2 [4]. The conduction band in the near surface region is almost flat compared with the un-doped GaN cap case. Several researchers investigated un-doped thin GaN cap layers to decrease gate leakage by the effect of piezoelectric and spontaneous polarization at GaN/AlGaN interface [9]. Maximum drain current was, however, low compared with the conventional structures due to reduced channel charge. In addition, it is relatively difficult to obtain good ohmic contact for un-doped thin

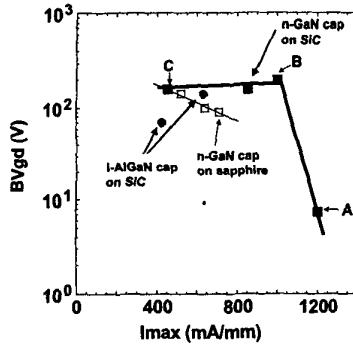


Fig. 4.  $\text{BV}_{gd}$  as a function of  $\text{Imax}$ . The effect of cap structures and substrates were investigated. Results of surface-charge-controlled N-GaN cap structures A, B, and C in Table I were also shown in this figure.

GaN cap layer. Here we suppress the surface charge effect on AlGaN and can obtain good ohmic contact with the n-type doped thin GaN cap layer.

Figure 3 shows off-state gate-drain breakdown voltage ( $\text{BV}_{gd-off}$ ) as a function of maximum drain current ( $\text{Imax}$ ) when sapphire substrates were used. Compared with a conventional AlGaN-cap structure, the surface-charge-controlled n-GaN-cap structure showed higher  $\text{BV}_{gd-off}$  of 140 V, defined as a  $\text{V}_{gd}$  at a gate current of 500  $\mu\text{A/mm}$ . N-GaN cap also screened surface traps.

### B. Surface-Charge-Controlled Structure on SiC

We compared three different thick n-AlGaN layers to control  $V_{th}$  as shown in Table I. We controlled  $V_{th}$  from -9 V to -2 V by changing AlGaN thickness. Structure A and B exhibited  $\text{BV}_{gd-off}$  of 160-200 V, When  $V_{th}$  became to -9 V (Structure A), however,  $\text{BV}_{gd-off}$  is less than 10 V. We introduced  $I_g$  measurement when  $\text{V}_{gd}$  is

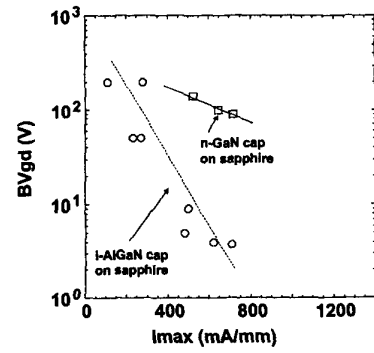


Fig. 3. Off-state breakdown voltage ( $\text{BV}_{gd-off}$ ) as a function of maximum drain current ( $\text{Imax}$ ) when sapphire substrates were used.

TABLE I  
SUMMARY OF DC CHARACTERISTICS

Structure No.	A	B	C
$V_{th}$ (V)	-9	-5.5	-2
$\text{Id}_{ss}$ at $\text{V}_g=0$ V (mA/mm)	980	750	300
$\text{Imax}$ at $\text{V}_g=2$ V (mA/mm)	1200	1000	450
$G_m$ -max (mS/mm)	150	180	230
$\text{BV}_{gd1}$ (V) at $\text{I}_{gd}=500$ $\mu\text{A/mm}$	7.5	>200	160-200
$\text{BV}_{gd2}$ (V) at $\text{I}_{gd}=1$ mA/mm	50	>200	160-200
$I_g$ -pinched-off ( $\mu\text{A/mm}$ ) at $\text{V}_{gd}=V_{th}$	810	60	25
$I_g$ ( $\mu\text{A/mm}$ ) at $\text{V}_{gd}=-50$ V	1000	90	65

settled to  $V_{th}$  (Table1). Gate leak current at  $V_{gd}$  of  $V_{th}$  increased, when  $V_{th}$  became negative. This is attributed to larger leakage through Schottky barrier till the 2DEG channel becomes pinched off state. This indicates that there is a limit of  $V_{th}$  even if the surface-charge-controlled structure is used.  $I_{max}$  decreased at structure C, suggesting that structure C with  $V_{th}$  of  $-2$  V is not sufficient for high power operation even if  $gm$  is large.

Figure 4 shows the dependence of  $BV_{gd-off}$  on maximum drain current. When n-GaN cap was used with SiC substrates, we could obtain high  $BV_{gd}$  with high drain current.  $BV_{gd}$  for SiC is larger compared with that of sapphire, suggesting that SiC is more promising to achieve high  $BV_{gd}$ .

#### C. DC and RF Characteristics ( $W_g=40-80 \mu m$ )

Figure 5 shows I-V characteristics measured by a 100 Hz curve-tracer. We compared the characteristics among different  $V_{th}$  of surface-charge-controlled structure. When  $V_{ds}$  was around 20 V, no current collapse was observed. When  $V_{ds}$  was around 50 V, however, current collapse occurred only for structure C (most positive  $V_{th}$ ). Only structure B showed high  $I_{max}$  and high  $BV_{gd}$  without current collapse. This suggests that current collapse occurred when  $V_{th}$  became positive. Electron

depletion thickness from surface may play an important role of current collapse.

Figure 6 shows transconductance ( $gm$ ) as a function of  $V_{gs}$ . DC- $gm$  and RF- $gm$  were compared to discuss  $gm$  dispersion. For structures A and B, DC- $gm$  and RF- $gm$  are almost same at the  $gm$  peak region, indicating that  $gm$  dispersion was suppressed by n-GaN cap layer. However, around  $V_g$  of 0 V, RF- $gm$  is larger than DC- $gm$ . This is mainly attributed to heat generation produced by high current density around 1A/mm. For structure C, DC- $gm$  and RF- $gm$  are the same at all  $V_{gs}$ . This is due to lower current density.

#### E. Power Characteristics ( $W_g=24 mm$ )

Figure 7 shows power characteristics at 2.2 GHz as a function of  $V_{ds}$ . Structure B and C were to estimate the effect of  $I_{max}$  and current collapse on power characteristics. We could operate 24-mm- $W_g$  HEMTs at 30 V. CW total output power increased till 30V without grinding a 400- $\mu m$ -thick SiC substrate. We obtained saturation power ( $Psat$ ) of 36 W at 30 V for structure B.  $P_{1dB}$  was over 30 W at 30 V.  $Psat$  for structure C is 2 dBm lower than structure B, which consistent to the difference of  $I_{max}$

Figure 8 shows CW power measurement results at 30 V.

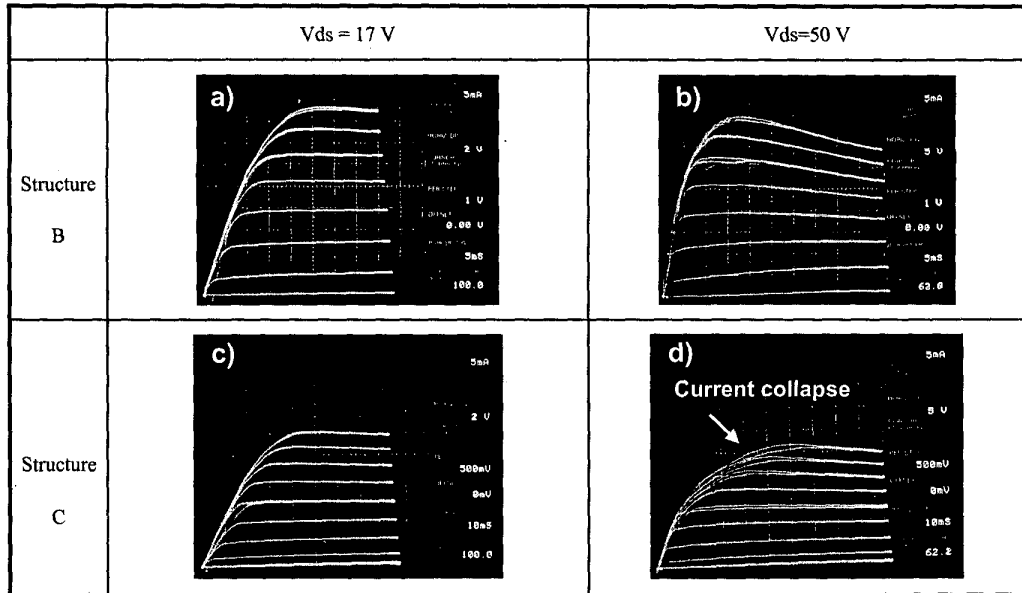


Fig. 5. Summary of  $Ids$ - $V_{ds}$  characteristics of two different surface-charge-controlled structures B and C. A gate width is  $40 \mu m$ . Vertical division is 5 mA. Horizontal division is 2 V for (a) and (c), and 5 V for (b) and (d). A gate voltage was varied from  $+2$  V to  $-5$  V by 1 V step for (a) and (b), and from  $+2$  V to  $-2$  V by 0.5 V step for (c) and (d). For structure C, current collapse occurred at 50 V operation at positive  $V_g$  region as shown in (d).

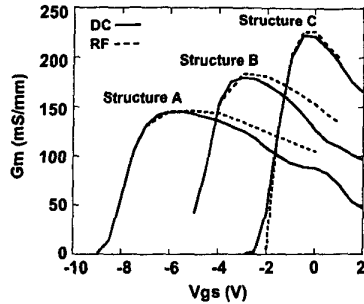


Fig. 6. Transconductance ( $g_m$ ) as a function of  $V_{gs}$  for different structures shown in Table I.  $W_g=80\ \mu\text{m}$ . Solid lines show DC- $g_m$  under DC measurement and dashed lines show RF- $g_m$  by S-parameter measurement. RF- $g_m$  is defined as an average  $g_m$  between 1 GHz and 3 GHz.

Linear gain of 9.7 dB with power added efficiency (PAE) of 29% was obtained for structure B. Structure C showed 10% lower PAE due to large current collapse.  $P_{out}$  for structure C was saturated at lower  $P_{in}$  compared structure B.

#### IV. CONCLUSION

In summary, we fabricated 24-mm-wide-gate AlGaN/GaN HEMTs using a surface-charge-controlled n-GaN-cap structure on SiC. We concluded that optimum  $V_{th}$  should be considered to obtain high  $BV_{gd}$  and to suppress current collapse. We demonstrate high voltage CW operation exhibiting high total output power of 36 W at 30 V. This high voltage operation with high current density was obtained only by optimizing  $V_{th}$  of surface-charge-controlled structure.

#### REFERENCES

- [1] Y-F Wu, D.Kpoplnek, J.P.Ibbetson, P.Parikh, B.P. Keller, and U.K.Mishra, "Very-High Power Density AlGaN/GaN HEMTs," *IEEE Trans. Electron. Devices*, Vol.48, pp586-590, March 2000.
- [2] Y.Ando, Y.Okamoto, H.Miyamoto, N.Hayama, T.Nakayama, K.kasahara, and M.Kuzuhara, " A 110-W AlGaN/GaN Heterojunction FET on Thinned Sapphire Substrates," *2001 IEDM Tech. Digest*, pp381-384, December 2001.
- [3] J.W.Palmour, S.T.Sheppard, R.P.Smith, S.T.Allen, W.L.Pribble, T.J.Smith, Z.Ring, J.J.Sumakeris, A.W.Saxler, and J.W.Miligan, "Wide Bandgap Semiconductor Devices and MMICs for RF Power Applications," *2001 IEDM Tech. Digest*, pp385-388, December 2001.
- [4] T.Kikkawa, N.Nagahara, N.Okamoto, Y.Tateno, Y.Yamaguchi, N.Hara, K.Joshin, and P.M.Asbeck, "Surface-Charge-Controlled AlGaN/GaN-Power HFET without Current Collapse and  $g_m$  Dispersion," *2001 IEDM Tech. Digest*, pp585-588, December 2001.
- [5] I.Daumiller, D.Theron, C.Caquiere, A.Vescan, R.Dietrich, A.Wieszt, H.Leier, "Current Instability in GaN-Based Devices," *IEEE Trans. Electron. Devices* vol.22, pp 62-64, Feb. 2001.
- [6] S.C.Binari, K.Ikossi, J.A.Roussos, W.Kruppa, D.Park, H.B.Dietrich, D.D.Koleske, A.E.Wickenden, and R.L.Henry, "Trapping Effects and Microwave Power Performance in AlGaN/GaN HEMTs," *IEEE Trans. Electron. Devices* Vol.48, pp465-471, March 2001.
- [7] R.Vetury, N.Q.Zhang, S.Keller, and U.K.Mishra, "The Impact of Surface States on the DC and RF Characterization of AlGaN/GaN HFETs," *IEEE Trans. Electron. Devices*. Vol.48, pp560-566, March 2001.
- [8] V.Tilak, B.Green, V.Kaper, H.Kim, T.Prunty, J.Smart, J.Shealy, and L. Eastman, "Influence of Barrier Thickness on High-Power Performance of AlGaN/GaN HEMTs," *IEEE Trans. Electron. Device Letters* vol.22, pp504-506, Nov. 2001.
- [9] X.Z.Dang, R.J.Welty, D.Qiao, P.M.Asbeck, S.S.Lau, E.T.Yu, K.S.Boutros, and J.M.Redwing, "Fabrication and Characterization of Enhanced Barrier AlGaN/GaN HEMT," *IEEE Electron. Lett.* Vol.35, pp602-603, April 1999.

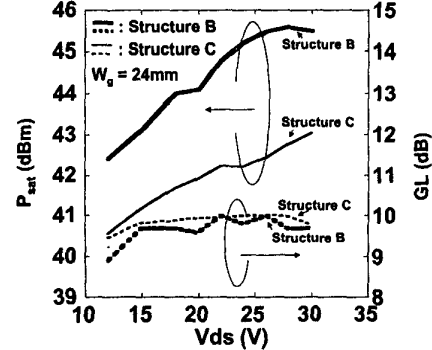


Fig. 7. CW power measurement results as a function of  $V_{ds}$ . Measured frequency is 2.2 GHz. Gate width is 24 mm. Packaged chip was measured.

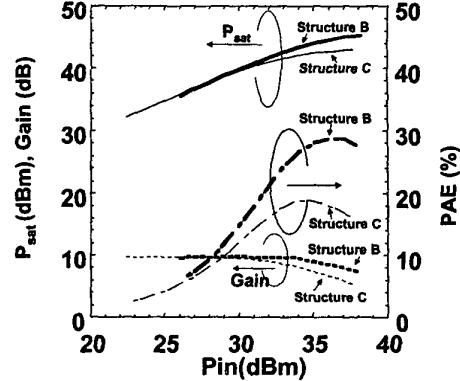


Fig. 8. CW power measurement results at 30 V as a function of  $P_{in}$ . Measured frequency is 2.2 GHz. Gate length is 0.9  $\mu\text{m}$ . Gate width is 24 mm. Packaged chip was measured.

1818